Drug–Polymer–Water Interaction and Its Implication for the Dissolution Performance of Amorphous Solid Dispersions

ARTICLE *in* MOLECULAR PHARMACEUTICS · DECEMBER 2014

Impact Factor: 4.38 · DOI: 10.1021/mp500660m · Source: PubMed

molecular pharmaceutics

Article

pubs.acs.org/molecularpharmaceutics

Drug–Polymer–Water Interaction and Its Implication for the Dissolution Performance of Amorphous Solid Dispersions

Yuejie Chen,[†] Chengyu Liu,[†] Zhen Chen,[†] Ching Su,[‡] Michael Hageman,[‡] Munir Hussain,[§] Roy Haskell,[∥] Kevin Stefanski,[‡] and Feng Qian*[,†]

[†]Department of Pharmacology and Pharmaceutical Sciences, School of Medicine, and Collaborative Innovation Center for Diagnosis and Treatment of Infectious Diseases, Tsinghua University, Beijing 100084, China

[‡]Pharmaceutical Candidate Optimization, Bristol-Myers Squibb Company, Lawrenceville, New Jersey 08648, United States

[§]Drug Product Science and Technology, Bristol-Myers Squibb Company, New Brunswick, New Jersey 08903, United States

[∥]Pharmaceutical Candidate Optimization, Bristol-Myers Squibb Company, Wallingford, Connecticut 06492, United States

ABSTRACT: The *in vitro* dissolution mechanism of an amorphous solid dispersion (ASD) remains elusive and highly individualized, yet rational design of ASDs with optimal performance and prediction of their *in vitro*/*in vivo* performance are very much desirable in the pharmaceutical industry. To this end, we carried out comprehensive investigation of various ASD systems of griseofulvin, felodipine, and ketoconazole, in PVP-VA or HPMC-AS at different drug loading. Physiochemical properties and processes related to drug–polymer–water interaction, including the drug crystallization tendency in aqueous medium, drug–polymer interaction before and after moisture exposure, supersaturation of drug in the presence of polymer, polymer dissolution kinetics, etc., were characterized and correlated with the dissolution performance of ASDs at different dose and different drug/polymer ratio. It was observed that ketoconazole/HPMC-AS ASD outperformed all other ASDs in various dissolution conditions, which was attributed to the drug's low crystallization tendency, the strong ketoconazole/HPMC-AS interaction and the robustness of this interaction against water disruption, the dissolution rate and the availability of HPMC-AS in solution, and the ability of HPMC-AS in maintaining ketoconazole supersaturation. It was demonstrated that all these properties have implications for the dissolution performance of various ASD systems, and further quantification of them could be used as potential predictors for *in vitro* dissolution of ASDs. For all ASDs investigated, HPMC-AS systems performed better than, or at least comparably with, their PVP-VA counterparts, regardless of the drug loading or dose. This observation cannot be solely attributed to the ability of HPMC-AS in maintaining drug supersaturation. We also conclude that, for fast crystallizers without strong drug–polymer interaction, the only feasible option to improve dissolution might be to lower the dose and the drug loading in the ASD. In this study, we implemented an ASD/water Flory–Huggins parameter plot, which might assist in revealing the physical nature of the drug–polymer interaction. We also introduced *supersaturation parameter* and *dissolution performance parameter* as two quantitative measurements to compare the abilities of polymers in maintaining drug supersaturation, and the dissolution performance of various solid dispersions, respectively.

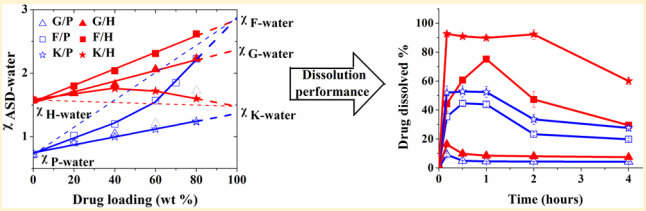

KEYWORDS: *amorphous solid dispersion, drug–polymer interaction, Flory–Huggins interaction parameter, dynamic vapor sorption, dissolution, FT-IR, NMR, crystallization*

INTRODUCTION

A successfully designed amorphous solid dispersion system (ASD) must possess two key characteristics: (1) physical stability during downstream processing and storage and (2) optimal dissolution performance upon *in vivo* dosing to achieve its desired bioavailability enhancement. In the past, there have been extensive studies focusing on the first area, and topics such as the thermodynamic aspects of amorphous small molecule,[1−10] the molecular interaction between drug and polymer,[11−14] crystallization of amorphous drugs in the presence of polymers,[15−17] the phase behavior of the binary drug–polymer systems,[18−22] etc. have been widely investigated and reviewed.

Satisfactory physical stability is only halfway toward the ultimate success of these thermodynamically metastable systems. We have demonstrated earlier that a physically stable ASD could have disappointing *in vivo* bioavailability performance, and ASDs of the same drug, same drug loading, yet different polymer carriers, could perform very differently *in vivo* despite their equally adequate physical stability in the dry state.[23] The poor *in vivo* performance predictability of the ASDs has become increasingly recognized as a touchy issue during

Received: October 2, 2014
Revised: December 18, 2014
Accepted: December 23, 2014
Published: December 23, 2014

DOI: 10.1021/mp500660m
Mol. Pharmaceutics 2015, 12, 576−589

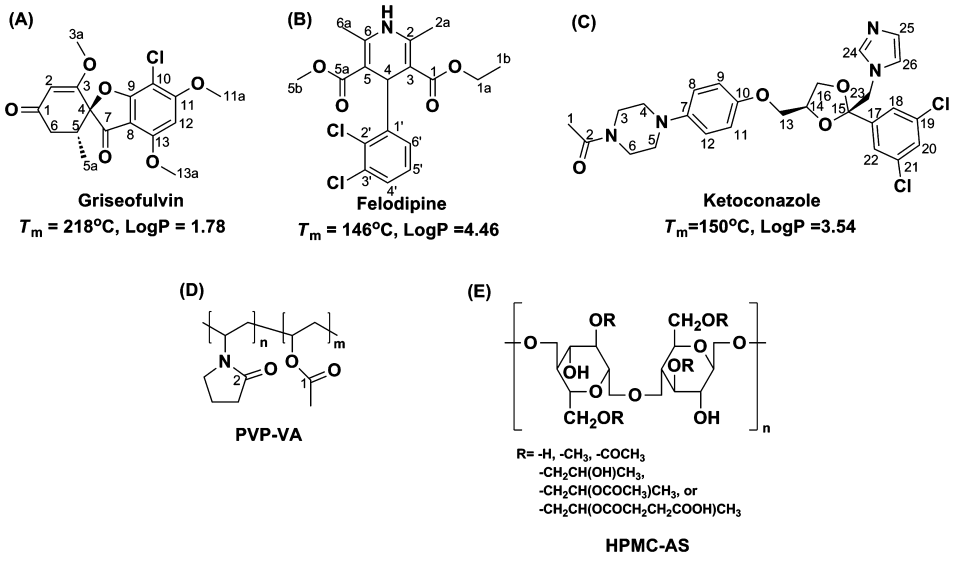

Figure 1. Chemical structure of model drugs, poly(vinylpyrrolidone-*co*-vinyl-acetate) (PVP-VA), and hydroxypropylmethylcellulose acetate succinate (HPMC-AS).

ASD development in the pharmaceutical industry,[24] and has been tackled by researchers in both academia and industry. Efforts such as development of biorelevant dissolution methods,[25] understanding of the solution behavior and dissolution performance of ASDs,[26,27] assessment of the crystallization tendency of amorphous drug in aqueous medium,[28−30] etc. have collectively advanced the knowledge in the field and will certainly contribute to a better prediction of the *in vivo* performance of ASDs and a more thoughtful and balanced strategy for ASD design.

Despite aforementioned efforts, prediction of the *in vitro* dissolution and *in vivo* bioavailability performance of an ASD remains challenging due to many interdependent physiochemical processes that occur simultaneously upon wetting of the formulation in an aqueous environment. Besides the dissolution of the amorphous drug from the ASD, the drug may also crystallize within the undissolved yet hydrated ASD,[23,31] and the drug−polymer interaction within the ASD might also change upon the hydration of the ASD.[18,19] The polymer dissolves from the ASD too, resulting in decreased polymer content within the hydrated ASD to stabilize the undissolved amorphous drug. The dissolved polymer could help to prolong the drug supersaturation and improve bioavailability,[23] through potential mechanisms such as formation of nanosized solution species with dissolved drug molecules.[25] Considering all these complications, apparently still lacking are experimental illustration of a complete picture of the dissolution process of ASDs (i.e., various changes occurring in the solution and the hydrated solids) and, furthermore, an in-depth understanding of the ternary interaction between drug, polymer, and water, potentially the ultimate decoder of the *in vitro* and *in vivo* performance of ASDs.

In this current work, we attempted to characterize the following aspects of the dissolution process of ASDs: (1) the dissolution kinetics of both the drug and the polymer; (2) the change of drug−polymer interaction upon contact of aqueous media; (3) the ability of polymers to prolong drug supersaturation, in the context of the amount of polymer dissolved into the dissolution media; and (4) the crystallization kinetics of the amorphous drug and ASD in aqueous environment. We also implemented a Flory−Huggins interaction parameter plot, wherein the ASD−water Flory−Huggins interaction parameters were plotted against the drug loading of the ASDs. It was observed that this plot, which intrinsically is a centralized summary of the ternary drug−polymer−water interaction, has apparent implications for the physical nature of drug−polymer interaction and the effect of water on the drug−polymer interaction. A *supersaturation parameter* was defined to quantify the ability of different polymers in maintaining drug supersaturation; and a *dissolution performance parameter* was defined to quantify the dissolution performance of different solid dispersions.

MATERIALS AND METHODS

Materials. Griseofulvin, felodipine, and ketoconazole were purchased from Beijing Ouhe Technology Co. Ltd. (Beijing, China). PVP-VA (Kollidon VA 64) was a gift from BASF Chemical Company Ltd. (Ludwigshafen, Germany). HPMC-AS was a gift from Shin-Etsu Chemical Co., Ltd. (Tokyo, Japan). The chemical structure and key physiochemical properties of the model compounds and polymers are summarized in Figure 1. All buffer salts used for dissolution medium, as well as methanol (HPLC grade) and acetone (HPLC grade) used for spray drying, were obtained from Beijing Chemical Works (Beijing, China).

Crystallization Tendency of Amorphous Drugs in FaSSIF. In order to assess the crystallization tendency of amorphous drugs in a biorelevant, aqueous medium, we used a polarized microscope (Zeiss Axio Imager A2m, Carl Zeiss, Germany) to study the crystallization kinetics of amorphous drugs immersed in fasted state simulated intestinal fluid (FaSSIF). The FaSSIF solution consists of 20 mM sodium phosphate (Na_2HPO_4), 47 mM potassium phosphate (KH_2PO_4), 87 mM sodium chloride (NaCl), 0.2 mM potassium chloride (KCl), 7.3 mM sodium taurocholate (NaTC), and 1.4 mM 1-palmitoyl-2-oleyl-*sn*-glycero-3-phosphocholine (POPC). The POPC was introduced as a solution in CH_2Cl_2, and then CH_2Cl_2 was removed by evaporation and sonication. The dissolution medium was adjusted to pH 6.5 with sodium hydroxide (NaOH).

DOI: 10.1021/mp500660m
Mol. Pharmaceutics 2015, 12, 576−589

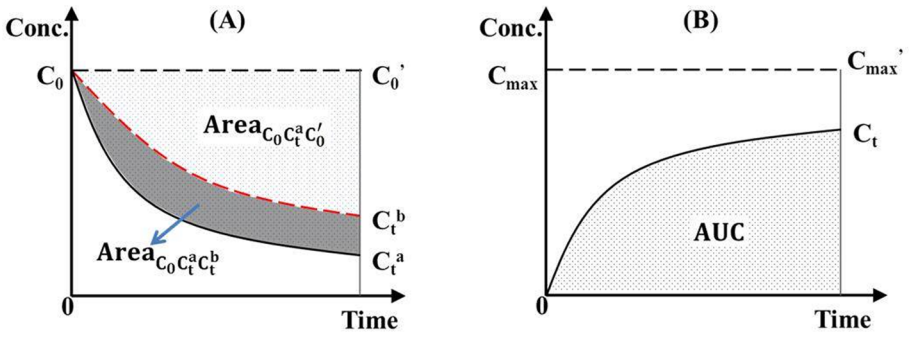

Figure 2. (A) Hypothetical illustration of the concentration−time curves of a drug supersaturated in a dissolution medium, with (curve $C_0C_t^b$) and without (curve $C_0C_t^a$) the presence of a polymer. The *supersaturation parameter* is defined as $\text{area}_{C_0C_t^aC_t^b}/\text{area}_{C_0C_t^aC_0'}$, where $\text{area}_{C_0C_t^aC_0'}$ is the integral area between curves $C_0C_t^a$ and C_0C_0', and $\text{area}_{C_0C_t^aC_t^b}$ is the integral area between curves $C_0C_t^a$ and $C_0C_t^b$. (B) A hypothetical dissolution profile of a solid dispersion. C_{max} is the maximal drug concentration if drug completely dissolved. The *dissolution performance parameter* is defined as $\text{AUC}_{actual}/\text{AUC}_{theoretical}$, where AUC_{actual} is the integral area under the curve C_0C_t, and $\text{AUC}_{theoretical}$ is the integral area under the curve $C_{max}C_{max}'$.

The amorphous drugs were made by a melt−quench process. Briefly, ∼20 mg of crystalline drug was placed on a glass slide and was melted in a hot-stage (Linkam LTS 420, Linkam Scientific Instrument Ltd., Surrey, U.K.) at 10 °C above the T_m of the drug. The temperature was maintained for ∼2−3 min to ensure complete melting. The glass slide with molten drug was then air cooled and immersed into FaSSIF solution at room temperature. The sample was withdrawn periodically and placed under the polarized microscope for qualitative assessment of the crystalline content.

Effect of Polymers on the Supersaturation of Amorphous Drugs in FaSSIF Solution. In order to assess the polymers' ability to maintain the supersaturation of drugs, PVP-VA or HPMC-AS was predissolved in FaSSIF at 0.3 and 3 mg/mL. DMSO solutions of model drugs were prepared at 100 or 20 mg/mL. To each 10 mL of polymer containing dissolution medium was added 100 μL of drug solution. The solution was then vibrated at a frequency of 100 rpm using a shaker (37 °C, Burrell wrist action shaker, model 75). After 0.3, 1, 2, and 4 h, the solution was centrifuged (13,000 rpm) for 3 min and the clear supernatant was analyzed for the concentration of drug using high performance liquid chromatography (HPLC) (Shimadzu LC-20AT; Kyoto, Japan). For comparison, the solubility of crystalline drugs in FaSSIF was determined by suspending excess amount of crystalline drugs in FaSSIF solution, followed by votexing (1 min), sonication (15 min), and then shaking for 24 h. The suspension was centrifuged at 13,000 rpm for 3 min, and the concentration of the supernatant was determined by HPLC/UV.

Figure 2A hypothetically illustrates the concentration−time curves of a drug supersaturated in a dissolution medium, with (curve $C_0C_t^b$) and without (curve $C_0C_t^a$) the presence of polymers, and curve C_0C_0' represents an ideal situation where drug remains solubilized in the medium and no drug precipitation occurred over the entire time period. To quantitatively compare the abilities of different polymers in maintaining and prolonging the drug supersaturation, *supersaturation parameter* was defined as eq 1:

$$\text{supersaturation parameter} = \frac{\text{area}_{C_0C_t^aC_t^b}}{\text{area}_{C_0C_t^aC_0'}} \quad (1)$$

where $\text{area}_{C_0C_t^aC_0'}$ is the integral area between curves $C_0C_t^a$ and C_0C_0' and can be conceptually considered as "the amount of drug precipitated from the solution over time" when no polymer was employed to maintain drug supersaturation. In the presence of polymer, curve $C_0C_t^a$ was elevated to $C_0C_t^b$, thus $\text{area}_{C_0C_t^aC_t^b}$, the integral area between curves $C_0C_t^a$ and $C_0C_t^b$, could be conceptually considered as "the amount of drug rescued from precipitation" by a certain type and amount of polymer. Apparently, *supersaturation parameter* is a dimensionless parameter between 0 and 1, where 0 indicates no supersaturation power at all while 1 indicates a complete inhibition of drug precipitation from solution. Practically, supersaturation parameter is a function of the drug structure, initial drug concentration, polymer type, and polymer concentration.

Preparation of Spray-Dried Amorphous Solid Dispersions. PVP-VA and HPMC-AS based amorphous solid dispersions of griseoflvin, felodipine, and ketoconazole were prepared by spray drying their ethanol solution (∼30 mg/mL) at a flow rate of ∼2 mL/min, using a Buchi spray dryer (B-90, Büchi Labortechnik AG, Postfach, Switzerland). For each drug−polymer system, solid dispersions with 20, 40, and 60 wt % drug loadings were prepared. The inlet temperature was 80−100 °C, and the outlet temperature was ∼40 °C. The spray-dried solid dispersions were placed under vacuum for at least 12 h to remove any residual solvents before further use. Glass transition temperature (T_g) of the solid dispersions was measured by DSC (TA DSC Q2000 differential scanning calorimeter, New Castle, DE). Briefly, approximately 5 mg of ASD samples was loaded into pin-holed, crimped aluminum pans. The sample was first heated to 105 °C and maintained for 5 min to remove any residual solvent, and scanned at 10 °C/min from 0 °C to ∼10 °C above the T_m of the drug. The middle point of the glass transition event was recorded as the T_g (Table 1).

***In Vitro* Dissolution Study under Nonsink Condition To Determine the Release Kinetics of the Drugs and the Polymers from the ASDs.** To achieve different sink conditions and different extents of drug supersaturation, ASD samples with 100 mg or 10 mg sample weights were loaded into 50 mL centrifuge tubes followed by addition of 20 mL of FaSSIF. The ASD samples were vortexed for 30 s prior to being placed on a shaker at 100 rpm. The samples were then centrifuged (13,000 rpm, 3 min) at times 0.2, 0.5, 1, 2, and 4 h, and then 2 mL of supernatant was withdrawn and analyzed for both the drug and the polymer concentration. Following each

DOI: 10.1021/mp500660m
Mol. Pharmaceutics 2015, 12, 576−589

Table 1. Glass Transition Temperature (T_g) of ASDs Prepared by Spray Drying

	T_g (°C)				
	drug	40% polymer	60% polymer	80% polymer	polymer
griseofulvin/PVP-VA	91.0	94.9	96.8	100.3	108.8
griseofulvin/HPMC-AS	91.0	86.6	88.4	95.8	121.0
felodipine/PVP-VA	47.0	69.3	83.0	95.8	108.8
felodipine/HPMC-AS	47.0	52.0	67.2	90.8	121.0
ketoconazole/PVP-VA	46.3	60.4	75.1	89.5	108.8
ketoconazole/HPMC-AS	46.3	58.7	75.5	97.2	121.0

sampling, the remaining ASDs were vortexed for 30 s and returned to the shaker to continue the dissolution experiment. The concentration of the drug in the supernatant was measured by HPLC with a UV spectrophotometer. Since PVP-VA and HPMC-AS do not show any useful UV absorption peaks, we developed an evaporative light scattering detector (ELSD) method for the analysis of their amount. Briefly, the supernatants were separated by a gradient method using HPLC (1260 series, Agilent Technologies, Santa Clara, CA, USA) with a polystyrene gel column (RS pak DS-413, 3.5 μm, 4.6 mm × 150 mm, Shodex, Japan) thermostated at 25 °C. Solvent A and solvent B used as the mobile phase are 1000/1 water/formic acid and 1000/1 acetonitrile/water, respectively. The polymer concentration was determined with an ELSD detector (380-LC, Agilent Technologies, USA) by comparing to a pre-established ELSD standard curve between polymer concentration and ELSD scattering intensity.

Figure 2B shows a hypothetical dissolution profile of a solid dispersion. C_{max} is the maximal drug concentration if entire amount of the drug dissolved in the dissolution medium. A higher AUC (area under the curve) of this dissolution profile indicates better dissolution performance, and the theoretical maximal AUC is defined by the AUC of line $C_{max}C_{max}'$, i.e., if drug reached the C_{max} immediately after the dosing, and was maintained constant over the dissolution time. In order to quantitatively compare the dissolution performance of various solid dispersions, we defined a *dissolution performance parameter* as follows:

$$\text{dissolution performance parameter} = \frac{\text{AUC}_{\text{actual}}}{\text{AUC}_{\text{theoretical}}} \quad (2)$$

where $\text{AUC}_{\text{actual}}$ is the integral area under the curve C_0C_t and $\text{AUC}_{\text{theoretical}}$ is the integral area under the curve $C_{max}C_{max}'$. Similarly to *supersaturation parameter* defined earlier, the *dissolution performance parameter* is a dimensionless parameter between 0 and 1, where 0 indicates completely no dissolution, while 1 indicates an ideal complete and prolonged dissolution process. Obviously, the *dissolution performance parameter* is a function of the drug, polymer, drug loading, dissolution condition, formulation properties, etc.

Determination of the Drug−Polymer Flory−Huggins Interaction Parameter. *Solubility of Crystalline Drugs in Polymers.* To determine the solubility of crystalline drug in polymers, an annealing method developed by the Lian Yu group was used.[32] Briefly, cryomilled drug−polymer mixtures were annealed at various temperatures to achieve phase equilibrium and then scanned by DSC at 10 °C/min to detect any residual drug crystals. For a drug−polymer mixture annealed at different temperatures, the method yields the upper and lower bounds for its equilibrium solution temperature.

Drug−Polymer Interaction Parameter. The Flory−Huggins model was used to obtain the drug−polymer interaction parameters. The drug activity at solubility can be calculated by eq 3, and the drug−polymer interaction parameter can be calculated by Flory−Huggins model shown in eq 4. A DSC scanning method was used to determine the following parameters.

$$\ln \alpha_d = \frac{\Delta H_m}{R}\left(\frac{1}{T_m} - \frac{1}{T}\right) \quad (3)$$

$$\ln \alpha_d = \ln \Phi_d + \left(1 - \frac{1}{x}\right)\Phi_p + \chi \Phi_p^{\,2} \quad (4)$$

where α_d is the drug activity, T_m is the melting temperature of pure drug, ΔH_m is the molar heat of fusion of pure drug, T is the solubility temperature, Φ_d is the volume fraction of the drug, Φ_p is the volume fraction of the polymer, x is the molar volume ratio of the polymer and the drug, and χ is the drug−polymer interaction parameter.

Determination of the ASD−Water Flory−Huggins Interaction Parameter. We prepared a series of ASDs with increasing drug loading from 0% (pure polymer), 20%, 40%, 60%, and 80%, by spray drying. The isothermal water absorption gravimetric curves of these ASDs were obtained using a dynamic vapor sorption apparatus (DVS Intrinsic, Surface Measurement Systems Ltd., London, U.K.). Assuming that the solution process is driven by a minimum free energy requirement, it can be shown in a form that gives the relative pressure of vapor as a function of vapor volume fraction absorbed:[33]

$$\ln(p/p_0) = \ln V_1 + \left(1 - \frac{1}{x}\right)V_2 + \chi V_2^{\,2} \quad (5)$$

where p is the partial pressure of gas, p_0 is the saturation pressure of the corresponding liquid at temperature T, V_1 is the volume fraction of the absorbed vapor, V_2 is the volume fraction of polymer or amorphous drug, and x is the relative molecular volume, taken to be infinity for the combination of a small molecule like water with a polymer. χ is the Flory−Huggins ASD−water vapor interaction parameter.

With the above approach, the Flory−Huggins interaction parameters between polymer and water and between ASD and water were determined. All ASD samples that underwent moisture absorption study were analyzed by DSC and PXRD to confirm if the samples remained amorphous after experiment. Although direct measurements were performed to obtained the Flory−Huggins interaction parameters between pure amorphous drug and water,[20,33,34] it is a risky approach due to the strong crystallization tendency of many pure amorphous drugs during the moisture absorption experiments. Therefore, in this study, we obtained the amorphous drug−water interaction parameters by extrapolating the drug loading in the ASD to 100% (Figure 3).

FT-IR Spectroscopic Study of ASDs before and after Their Exposure to High Moisture. To understand the effects of moisture on the drug−polymer interaction, IR spectra of ASDs were collected by Fourier transform infrared spectros-

DOI: 10.1021/mp500660m
Mol. Pharmaceutics 2015, 12, 576−589

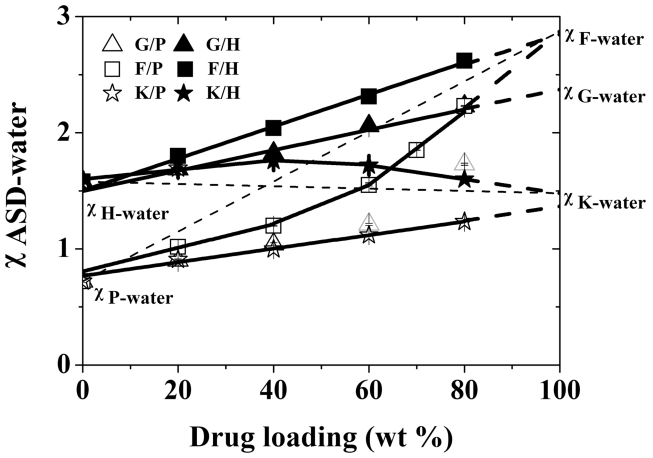

Figure 3. Flory–Huggins interaction parameters between ASDs and water. By extrapolation to pure drug, the interaction parameters between amorphous drugs and water were obtained. The dashed lines in the F/P and K/H systems indicate the theoretical value if the drug and polymer were mixed physically. (G, griseofulvin; F, felodipine; K, ketoconazole; P, PVP-VA; H, HPMC-AS).

copy (Vertex 70, Bruker Optics, Ettlingen, Germany) with a spectral resolution of 4 cm^{-1}. The IR spectra in the wave numbers in the range 4000–700 cm^{-1} were recorded for further comparison. The ASDs were then exposed to high humidity condition (25 °C/100% RH) generated by a dynamic vapor sorption apparatus (DVS Intrinsic, Surface Measurement Systems Ltd., London, U.K.), for 4 h at a gas flow rate of 200 mL/min. The ASDs were then dried in dry air (RH < 2% at 25 °C) until a plateau in the weight loss was observed (approximately 12 h). The IR spectra of the dried ASD samples were again collected. As a control, the IR spectra of pure amorphous drugs and polymers were also obtained.

Solution NMR. In order to understand the molecular mechanism of drug–polymer interaction, the drugs alone and the 40/60 (w/w) drug/polymer were dissolved in deuterochloroform, and their ^{13}C NMR spectra were obtained at room temperature using a Bruker AV-400 (Bruker BioSpin GmbH, Rheinstetten, Germany) NMR operating at 100 MHz. The deuterochloroform solvent signal was used as the reference ($CDCl_3$, 77.160 ppm). Spectral assignments for felodipine and ketoconazole were accomplished according to literature reports.[35,36]

RESULTS AND DISCUSSION

Crystallization Tendency of the Amorphous Griseofulvin, Felodipine, and Ketoconazole in Aqueous Environment. The crystallization tendency of pure amorphous griseofulvin, felodipine, and ketoconazole immersed in FaSSIF solution is compared in Figure 4. Crystallization of amorphous griseofulvin occurred rapidly within 10 min, and the crystallization on the surface of amorphous griseofulvin completed within 30 min. In contrast, amorphous felodipine and ketoconazole crystallized much more slowly in FaSSIF solution. Amorphous felodipine did not crystallize in FaSSIF solution within 2 h, and only a fraction of amorphous felodipine crystallized after 4 h; while amorphous ketoconazole remained amorphous in FaSSIF after 4 h.

Different crystallization tendency of amorphous griseofulvin, felodipine, and ketoconazole in FaSSIF solution could certainly be attributed largely to their molecular configuration, which could be confirmed by their crystallization tendency in the dry state[37] and is also consistent with some thermodynamic analysis of these compounds.[4,38] Water wetting and plasticizing could be the other critical factors to accelerate the drug crystallization. Water is a well-known plasticizer due to its low T_g at −108 °C.[39] Compared with felodipine (Log P = 4.46) and ketoconazole (Log P = 3.54), the less lipophilic griseofulvin

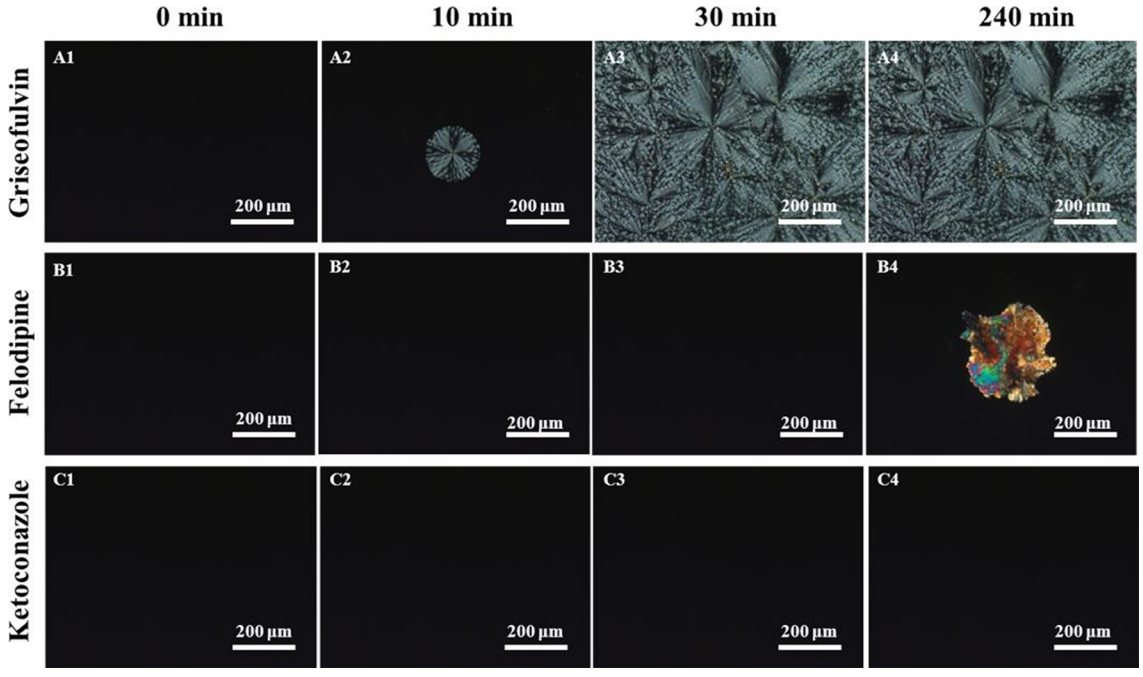

Figure 4. Crystallization kinetics of amorphous drugs upon submerging into FaSSIF solution: (A) griseofulvin; (B) felodipine; (C) ketoconazole. (Felodipine did not crystallize after 2 h.)

DOI: 10.1021/mp500660m
Mol. Pharmaceutics 2015, 12, 576–589

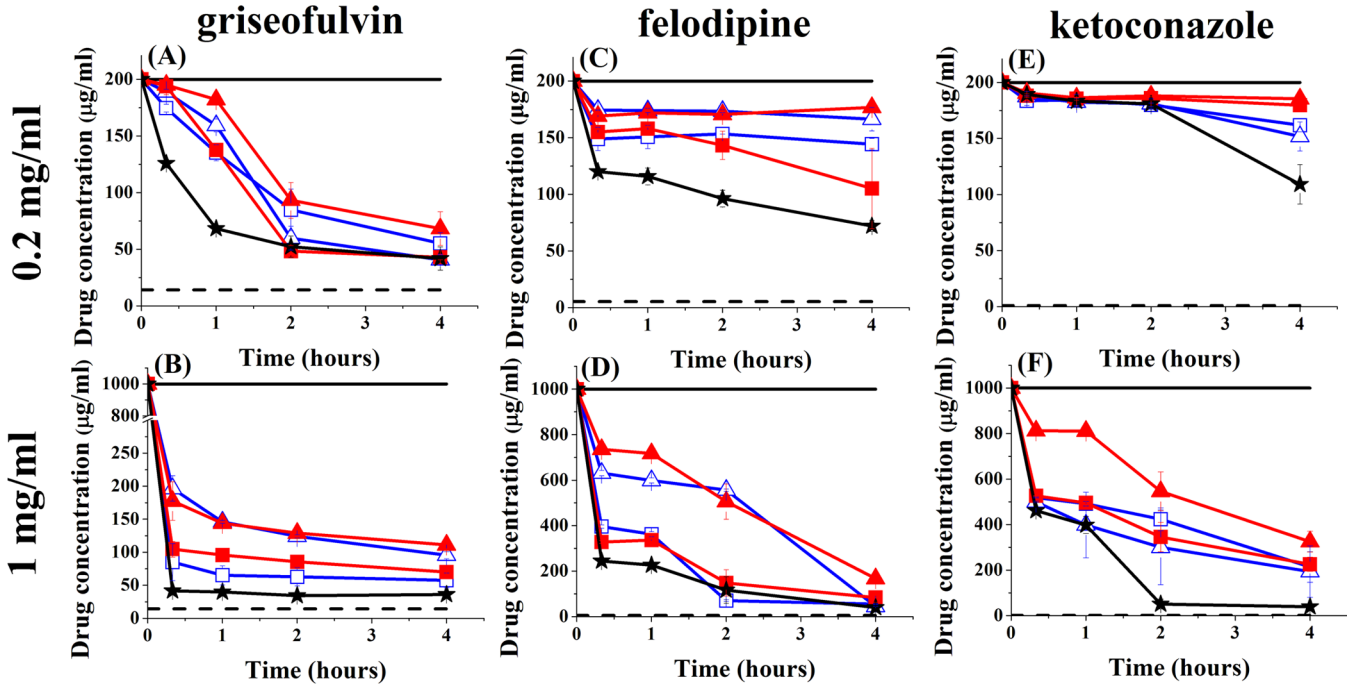

Figure 5. Effect of HPMC-AS and PVP-VA on the supersaturation of model drugs. The initial supersaturated drug concentration is 0.2 or 1 mg/mL as illustrated by the solid line at the top; the solubility of crystalline drug in the dissolution medium without polymer is illustrated by the dashed line at the bottom (n = 3 for all experiments) (— initial supersaturation; – – – crystalline drug solubility; blue □, 0.3 mg/mL PVP-VA; blue △, 3 mg/mL PVP-VA; red ■, 0.3 mg/mL HPMC-AS; red ▲, 3 mg/mL HPMC-AS; black ★, without polymer).

(Log P =1.78) favors water absorption, which might have also contributed to its rapid crystallization.

Supersaturation of Griseofulvin, Felodipine, and Ketoconazole in the Presence of PVP-VA and HPMC-AS. During the dissolution of ASDs, both the drug and the polymer dissolve, and the polymer concentrations in the dissolution media are variable. Therefore, it is necessary to assess the polymers' ability in prolonging drug supersaturation when different concentrations of polymer are present. Hypothetically, if a solid dosage form of interest contains 750 mg of stabilizing polymer (i.e., assume you have a big ASD tablet), and the fluid volume in the GI tract is 250 mL, 10% or 100% polymer release will generate a polymer concentration of 0.3 or 3 mg/mL, respectively. In this study, we consider 0.3 mg/mL as a low polymer concentration presumably achieved during the beginning stage of dissolution, while we consider 3 mg/mL as a high polymer concentration that occurs at the later stage of dissolution. We compared the ability of predissolved PVP-VA and HPMC-AS in prolonging the supersaturation of griseofulvin, felodipine, and ketoconazole, using polymer concentrations of 0.3 and 3 mg/mL. With different drug doses, drug loading, and drug release rates, different extent of drug supersaturation exists in the dissolution media. Assuming a dosage form of 250 mg of active pharmaceutical ingredient and, again, a 250 mL GI fluid volume, 20% of drug dissolution and 100% of drug dissolution will yield 0.2 and 1 mg/mL of drug concentration. Considering this, we selected two initial supersaturation levels for the model drugs, at 0.2 or 1 mg/mL, respectively, as illustrated by the solid lines on top of the plots in Figure 5. The equilibrium solubility of crystalline model drugs is illustrated by the dashed line at the bottom of the plots in Figure 5.

Concentration–time plots of initially supersaturated 0.2 or 1 mg/mL griseofulvin, felodipine, and ketoconazole, in the presence of 0.3 or 3 mg/mL PVP-VA and HPMC-AS, were collected over 4 h (Figure 5). We summarize the behavior of each drug as follows.

Griseofulvin. At 0.2 mg/mL drug supersaturation (Figure 5A), both HPMC-AS and PVP-VA delayed the drug precipitation in the initial 2 h. Higher concentration of HPMC-AS at 3 mg/mL is slightly more effective than a lower concentration of HPMC-AS at 0.3 mg/mL, while different concentration of PVP-VA did not show significant difference in maintaining griseofulvin supersaturation. Comparing the two polymers, the ability of maintaining griseofulvin supersaturation appears to be similar. At an elevated drug supersaturation at 1 mg/mL (Figure 5B), neither polymer could prevent the rapid drug precipitation. However, the drug concentration reached plateaus higher than the crystalline drug concentration after 1 h, and the concentration of the plateaus is polymer concentration dependent while not dependent on polymer type, i.e., 3 mg/mL polymers, regardless of HPMC-AS or PVP-VA, maintained a higher griseofulvin supersaturation at ~100–150 μg/mL, compared with griseofulvin supersaturation at ~50–100 μg/mL, when only 0.3 mg/mL of polymers were present.

Griseofulvin has weak Flory–Huggins interaction with both PVP-VA and HPMC-AS, with Flory–Huggins interaction parameters at −0.14 and 0.26 (Table 2), respectively. Furthermore, the relative hydrophilic (Log P = 1.78) nature favors its interaction with water to facilitate the crystallization. Both situations may lead to a weak adsorption of polymers to the drug crystal surface, resulting in a compromised inhibition effect on drug precipitation rates.

Felodipine. At 0.2 mg/mL drug supersaturation (Figure 5C), 0.3 mg/mL of either HPMC-AS or PVP-VA could elevate the drug supersaturation from ~80–120 μg/mL to ~110–150 μg/mL within 4 h, while increasing the polymer concentration to 3

DOI: 10.1021/mp500660m
Mol. Pharmaceutics 2015, 12, 576–589

Table 2. Flory–Huggins Interaction Parameters between Drug, Polymer, and Water

interaction parameters	PVP-VA	HPMC-AS	water
griseofulvin	−0.14	0.26	2.37[b]
felodipine	−1.9	−0.21	2.87[a] (2.85[b])
ketoconazole	−0.43	−1.68	1.37[a] (1.48[b])
water	0.72	1.58	N/A

[a]Extrapolated from PVP-VA based solid dispersions. [b]Extrapolated from HPMC-AS based solid dispersions.

mg/mL slightly increased the drug supersatruation further to ∼175 μg/mL. HPMC-AS and PVP-VA did not show statistically significant difference in maintaining felodipine supersaturation. When the drug supersaturation was increased to 1 mg/mL (Figure 5D), only higher concentration of polymer at 3 mg/mL could delay the rapid drug precipitation and increase drug supersaturation, while lower polymer concentration at 0.3 mg/mL, regardless of the polymer type, appeared to have little effect in prolonging the supersaturation of felodipine.

It is worth noting that, in the dry state, felodipine interacts with PVP-VA much more strongly than with HPMC-AS, demonstrated by Flory–Huggins interaction parameters of felodipine/PVP-VA and felodipine/HPMC-AS at −1.9 and −0.21, respectively (Table 2). On the other hand, it is well-known that factors such as drug–polymer hydrogen bond interaction, drug–polymer hydrophobic interaction, steric hindrance of polymer, the solution viscosity, et al. could all affect the drug precipitation from supersaturation.[40] Although the physical interaction between felodipine and PVP-VA is much stronger than that between felodipine and HPMC-AS, the more hydrophilic property of PVP-VA could reduce its interaction with hydrophobic drugs in the aqueous medium, thus to negate its ability to maintain drug supersaturation in solution.

Ketoconazole. As a slow crystallizer (Figure 4), supersaturated ketoconazole precipitates slowly. At 0.2 mg/mL drug supersaturation (Figure 5E), the drug supersaturation was more prolonged particularly between 2 and 4 h with either PVP-VA or HPMC-AS, while HPMC-AS is more effective than PVP-VA. For both polymers, when the concentration in the dissolution medium was increased from 0.3 mg/mL to 3 mg/mL, the drug supersaturation was similar without further increasing, presumably because ketoconazole already reached a high supersaturation even without polymer or with low concentration of polymer. When the supersaturation of ketoconazole was increased to 1 mg/mL (Figure 5F), 3 mg/mL of HPMC-AS demonstrated superior capability in maintaining ketoconazole supersaturation, compared with 0.3 mg/mL of HPMC-AS or PVP-VA, and 3 mg/mL of PVP-VA, where none of the above was able to prevent the precipitation of high concentration of ketoconazole, or to prolong the supersaturation.

Apparently, the interaction between ketoconazole and HPMC-AS (−1.68) is much stronger than that between ketoconazole and PVP-VA (−0.43). The hydrophobic nature of ketoconazole (Log P = 3.54) could also favor its interaction with HPMC-AS in the solution state. A higher HPMC-AS concentration at 3 mg/mL was also more capable of maintaining ketoconazole supersaturation with an initial 1 mg/mL concentration. Presumably, the greater steric hindrance of the polymer could have prevented the crystallization of amorphous ketoconazole in solution.

Flory–Huggins Interactions between Drug, Polymer, and Water. The Flory–Huggins interaction parameters between the drug, polymer, and water are summarized in Table 2. As explained in Materials and Methods, the interaction parameters between drug and polymer and between polymer and water are determined directly, while that between amorphous drug and water was obtained by extrapolation (Figure 3).

Drug–Polymer Flory–Huggins Interaction. According to the Flory–Huggins free energy of mixing,[41,42] a negative interaction parameter between the drug and the polymer indicates that the amorphous drug is completely miscible with the polymer, while a large positive interaction parameter indicates the immiscibility of the drug and the polymer. The more negative Flory–Huggins interaction parameters imply stronger drug–polymer interaction, which eventually contributes to the negative free energy of mixing at any drug–polymer ratio. All three model drugs appear to be completely miscible thermodynamically with both PVP-VA and HPMC-AS in the dry state due to their negative Flory–Huggins parameters, except for the griseofulvin/HPMC-AS system that could only have a marginal miscibility, due to a slightly positive χ value between griseofulvin and HPMC-AS. Among all drug/polymer systems, the felodipine/PVP-VA and ketoconazole/HPMC-AS systems have strong interaction due to their large negative interaction parameters at −1.9 and −1.68.

Polymer–Water Flory–Huggins Interaction. The sorption isotherms of water vapor in PVP-VA and HPMC-AS are linear at low vapor activities (a < 0.4 for HPMC-AS and a_w < 0.3 for PVP-VA) and increase exponentially at higher vapor activities (data not shown). PVP-VA absorbed much more water than HPMC-AS; applying these sorption data to eq 5, Flory–Huggins interaction parameter between polymer and water can be calculated. In this work, we used the interaction parameter at 100% RH for further discussion, i.e., 0.72 for PVP-VA/water and 1.58 for HPMC-AS/water, as 100% RH is approaching the aqueous dissolution medium (Table 2).

ASD–Water Flory–Huggins Interaction. The interaction parameters between ASDs and water were determined, and the amorphous drug–water interaction parameters were obtained by extrapolation method (Figure 3 and Table 2). Among the six ASD systems between the drugs (griseofulvin, felodipine, ketoconazole) and the polymers (PVP-VA and HPMC-AS), ASDs of felodipine and ketoconazole, regardless of polymer carrier and drug loading, remained amorphous after the water sorption experiments. However, as a fast crystallizer, although griseofulvin was found to be able to remain amorphous in HPMC-AS in all drug loadings after water sorption, it crystallized within PVP-VA at drug loadings above 40%. Therefore, this method is not applicable for griseofulvin/PVP-VA ASDs at high drug loading.

In Figure 3, we plotted the ASD–water Flory–Huggins interaction parameters, $\chi_{ASD-water}$, over the drug loading in ASD. Interestingly, for felodipine/HPMC-AS, griseofulvin/HPMC-AS, and ketoconazole/PVP-VA systems, their $\chi_{ASD-water}$ plots remained linear over the whole range of drug loading, and the ASD–water interaction parameters appeared to be equivalent to the linear addition of that between water and pure amorphous drug, and that between water and pure polymer. We believe that this phenomenon is consistent with the weak interaction within these ASDs, which was revealed by their slightly negative or positive Flory–Huggins interaction parameters (Table 2).

DOI: 10.1021/mp500660m
Mol. Pharmaceutics 2015, 12, 576–589

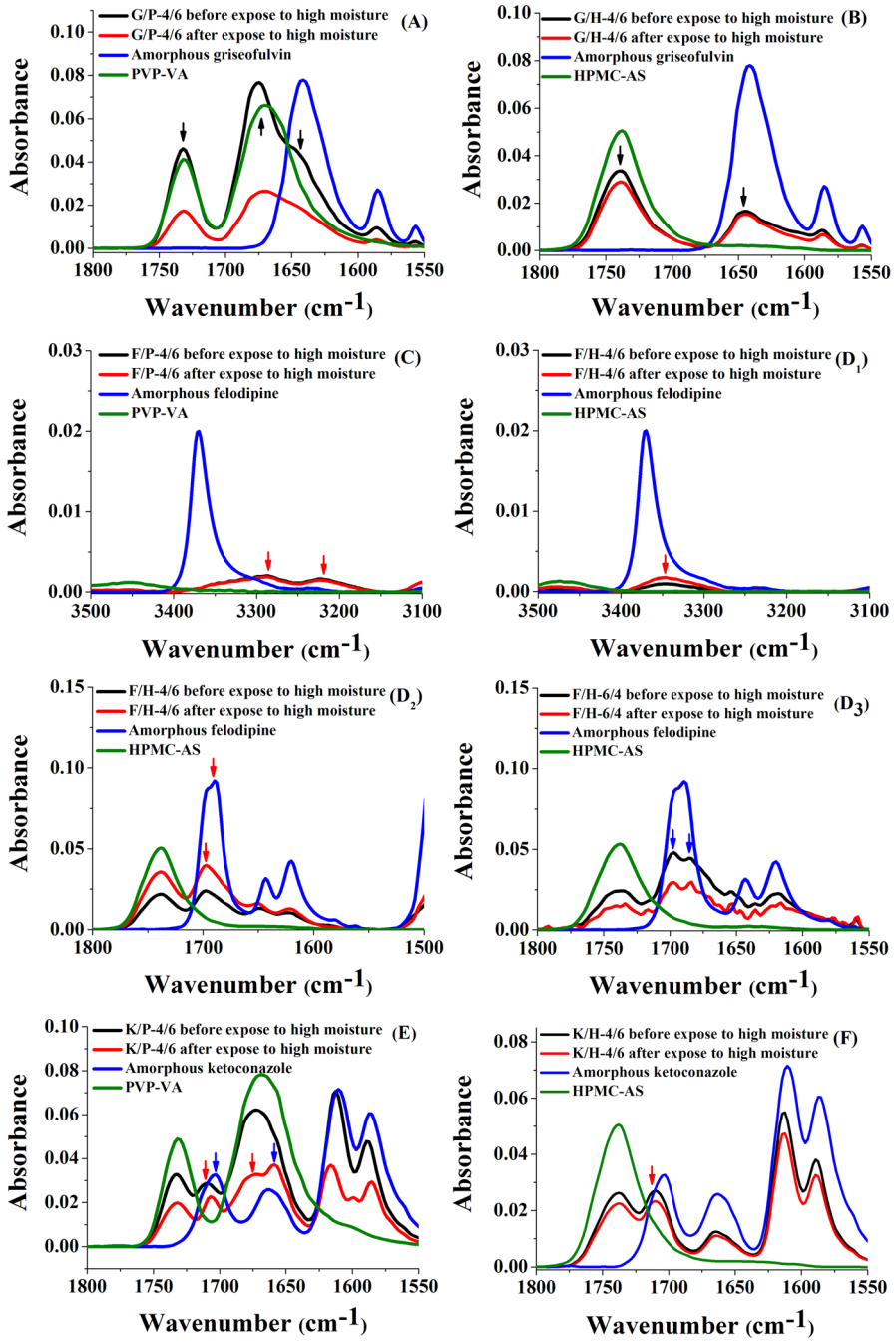

Figure 6. IR spectra of (A) the carbonyl region of 40/60 griseofulvin/PVP-VA, (B) the carbonyl region of 40/60 griseofulvin/HPMC-AS, (C) the −NH region of 40/60 felodipine/PVP-VA, where the red arrows show *ν*NH of amorphous felodipine without C═O bonding, (D_1) the −NH region of 40/60 felodipine/HPMC-AS, (D_2) the carbonyl region of 40/60 felodipine/HPMC-AS, (D_3) the carbonyl region of 60/40 felodipine/HPMC-AS, (E) the carbonyl region of 40/60 ketoconazole/PVP-VA, and (F) the carbonyl region of 40/60 ketoconazole/HPMC-AS. (Pure amorphous drug: blue. Polymer: pink. ASD before and after moisture exposure: black and red.)

The felodipine/PVP-VA and ketoconazole/HPMC-AS systems showed nonlinear $\chi_{ASD-water}$ vs drug loading plots, presumably caused by the strong drug−polymer interaction in these two systems. An apparent difference between these two nonlinear plots is that the felodipine/PVP-VA system displayed a negative deviation from the linear addition of PVP-VA−water interaction and amorphous felodipine−water interaction; while the ketoconazole/HPMC-AS system displayed a positive deviation from the linear addition. Although the molecular mechanism behind this is still under investigation in our lab, this observation suggests that, effectively, the felodipine/PVP-VA interaction makes the ASD more hydrophilic than the physical blend of amorphous felodipine and PVP-VA, while the ketoconazole/HPMC-AS interaction makes the ASDs more hydrophobic than the physical blend of amorphous ketoconazole and HPMC-AS. As demonstrated later by the FT-IR spectroscopic study (Figure 6), the drug−polymer interaction within both felodipine/PVP-VA and ketoconazole/HPMC-AS systems survived the moisture exposure. The $\chi_{ASD-water}$ vs drug loading plot is not applicable for the griseofulvin/PVP-VA ASD due to the crystallization of griseofulvin within PVP-VA during the experiment. Another interesting observation is, regardless of

DOI: 10.1021/mp500660m
Mol. Pharmaceutics 2015, 12, 576−589

Table 3. Chemical Shifts in ^{13}C NMR Spectrum of Model Drug−Polymer Systems

	Δδ ^{13}C			Δδ ^{13}C			Δδ ^{13}C	
C no.	G/P	G/H	C no.	F/P	F/H	C no.	K/P	K/H
1	−0.021	0.075	C_{5a}	−0.02	−0.036	2	−0.053	**0.158**
7	−0.047	0.054	C_{3a}	−0.025	−0.043	10	−0.084	0.007
3	−0.021	0.046	C_1'	0.086	−0.003	7	−0.094	−0.016
9	−0.052	0.046	C_6	**0.17**	**−0.12**	24	−0.097	**−0.16**
11	−0.037	0.024	C_2	**0.172**	**−0.119**	18	−0.095	0.076
13	−0.043	0.029	C_3'	−0.073	0.036	17	−0.092	−0.131
8	−0.064	0.05	C_6'	−0.058	0.057	20	−0.091	0.008
2	−0.063	0.047	C_2'	−0.015	0.032	19	−0.095	0.036
10	−0.063	0.058	C_4'	−0.079	0.028	22	−0.069	0.026
4	−0.06	0.05	C_5'	−0.045	0.016	25	**−0.172**	**−0.808**
12	−0.039	0.005	C_3	**−0.158**	**0.13**	21	−0.081	0.041
11a	−0.045	0.017	C_5	**−0.161**	**0.129**	26	−0.067	**0.125**
3a	−0.045	0.039	3b	−0.097	0.02	8	−0.085	0.036
13a	−0.049	0.02	5b	−0.078	0.023	12	−0.085	0.036
6	−0.065	0.028	4	−0.057	0.015	9	−0.079	0.008
5	−0.063	0.036	2a	**−0.129**	**0.113**	11	−0.079	0.008
5a	−0.06	0.031	6a	**−0.127**	**0.116**	15	−0.096	−0.101
			3c	−0.027	0.023	14	−0.086	0.012
			PVP-VA			13	−0.079	−0.016
			2	−0.043		16	−0.102	−0.028
			1	**0.1**		23	−0.081	0.116
						4	−0.09	0
						5	−0.094	0.002
						3	−0.085	0.001
						6	−0.08	0.033
						1	−0.09	−0.036
						PVP-VA		
						2	**−0.104**	
						1	+0.061	

[a]Chemical shifts that show substantial changes due to drug-polymer interaction are highlighted in bold.

polymer carrier, when the $\chi_{ASD-water}$ of felodipine ASDs and ketoconazole is extrapolated to 100% drug loading, the same $\chi_{drug-water}$ values were obtained, which further validated this approach.

FT-IR Spectroscopic Investigation of the Hydrogen Bonding within the ASDs before and after Moisture Exposure. A single T_g with a value between those of the pure drug and the pure polymer was detected by DSC in all the ASD systems obtained shortly after spray drying (Table 1), indicating the molecular level mixing in these ASDs. To understand the mechanism of drug−polymer interaction before and after moisture exposure, ASDs of 40% drug loading were exposed to moisture; FT-IR was used to analyze the hydrogen bonding between drug and polymer, before and after moisture exposure (Figure 6).

Figures 6A and 6B showed the carbonyl region of the griseofulvin/PVP-VA and griseofulvin/HPMC-AS ASDs. No peak shift was observed between the ASDs and the pure components, and the FT-IR spectra of the two ASDs are basically the linear addition of the spectra of the pure amorphous griseofulvin and polymers weighted by each component's content. This observation is consistent with the weak Flory−Huggins interaction between griseofulvin and either polymer, which collectively suggest the absence of H-bonding between griseofulvin and the polymers.

For the amorphous felodipine, two FT-IR peaks centered at 3370 and 3286 cm^{-1} were assigned to the −NH moiety of the drug, while in the felodipine/PVP-VA ASD, these two peaks shifted to 3329 and 3223 cm^{-1}, respectively (Figure 6C), which was attributed to the drug−polymer H-bonding formation between the NH moiety and PVP-VA. Interestingly, this hydrogen bonding within the felodipine/PVP-VA ASD was not disrupted by moisture exposure. This is also consistent with the observation of the strong Flory−Huggins interaction between drug and polymer (Table 2). In the 40% drug loading felodipine/HPMC-AS ASD, the NH moiety peaks centered at 3370 cm^{-1} shifted slightly to 3346 cm^{-1} (Figure 6D$_1$), suggesting the formation of weak drug−polymer H-bonding through the NH moiety of felodipine. Meanwhile, felodipine can also form another type of specific interaction with HPMC-AS (Figure 6D$_2$), as NMR results showed (detailed discussion in the next section). In the FT-IR results (Figure 6D$_2$), two peaks centered at 1697 and 1690 cm^{-1} were assigned respectively to the free carbonyl of felodipine, and the same carbonyl moiety when intermolecular hydrogen bonding occurs between the drug molecules. The intensity ratio between these two peaks remained unchanged in the 40% drug loading ASD before and after its exposure to 100% RH for 4 h (Figure 6D$_2$). However, the intensity ratio between the 1690 cm^{-1} peak and the 1697 cm^{-1} peak of the 60% ASD increased after moisture exposure (Figure 6D$_3$), suggesting that moisture exposure might have disrupted the felodipine/HPMC-AS interaction, while increasing the amount of free felodipine and intermolecular hydrogen bonding between felodipine molecules.

DOI: 10.1021/mp500660m
Mol. Pharmaceutics 2015, 12, 576−589

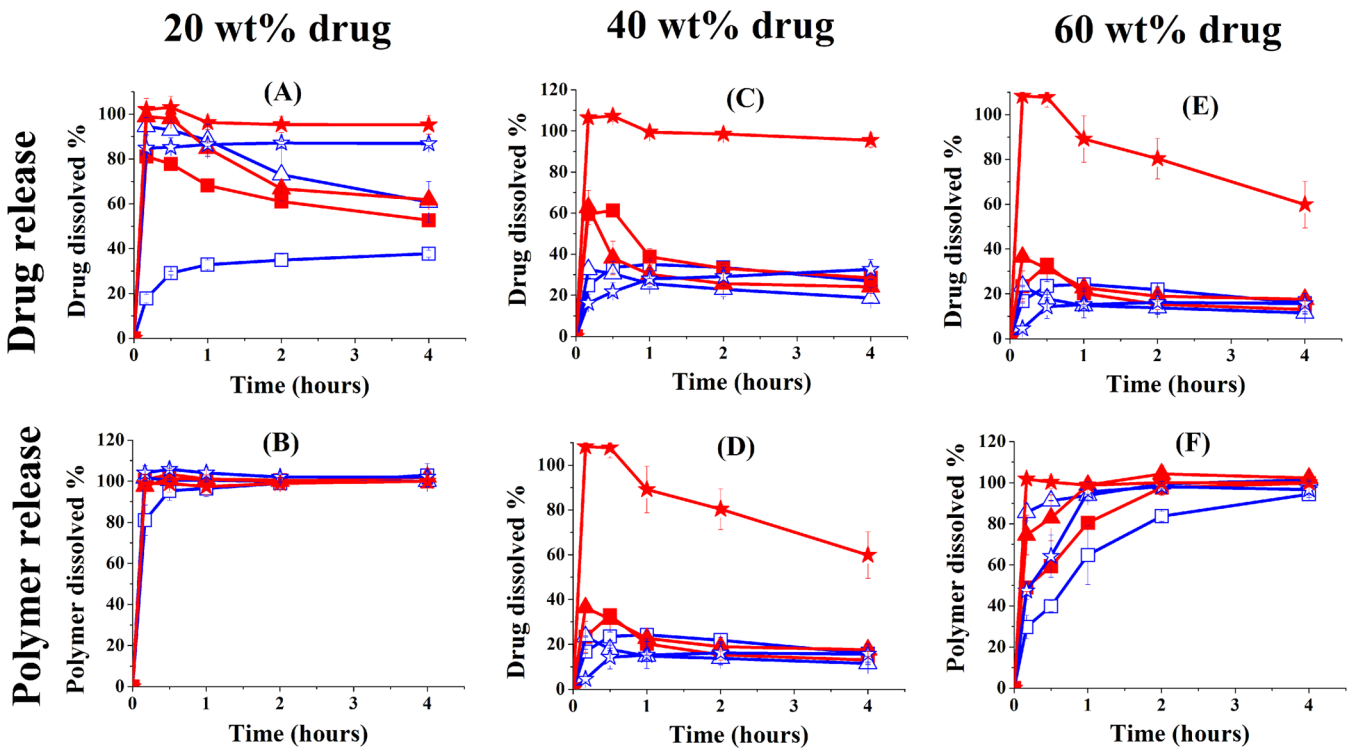

Figure 7. Dissolution of ASDs in FaSSIF solution at the ASD concentration of 0.5 mg/mL. Both drug and polymer release profiles were measured and are listed on the top (A, C, E) and bottom (B, D, F) panels, respectively. The profiles are arranged according to the drug loading in the ASDs: (A, B) ASD with 20% drug loading; (C, D) ASD with 40% drug loading; (E, F) ASD with 60% drug loading (n = 3 for all experiments) (blue △, G/P ASD; red ▲, G/H ASD; blue □, F/P ASD; red ■, F/H ASD; blue ☆, K/P ASD; red ★, K/H ASD).

According to the Flory–Huggins parameter, ketoconazole interacts moderately with PVP-VA (interaction parameter: −0.43). NMR results also indicated the existence of ketoconazole/PVP-VA interaction (to be discussed later). In the FT-IR spectrum of the ketoconazole/PVP-VA ASD, two peaks at 1709 and 1672 cm^{-1} were assigned to the free carbonyl moiety of ketoconazole. These two peaks slightly shift to 1707 and 1666 cm^{-1}, respectively, after exposure to 100% RH for 4 h (Figure 6E). The shifted peaks overlap with those of pure amorphous ketoconazole, suggesting the disruption of ketoconaozole/PVP-VA interaction by moisture. The moderate ketoconazole/PVP-VA interaction, as well as the hydrophilicity of PVP-VA, might have facilitated the moisture penetration and eventually the competitive disruption of the ketoconaozole/PVP-VA interaction by water.

Three IR peaks were observed in the ketoconazole/HPMC-AS system, between 1650 and 1800 cm^{-1} (Figure 6F). Due to the ketoconazole/HPMC-AS interaction, the 1714 cm^{-1} (carbonyl of ketoconazole) shifted from its peak position in the pure amorphous ketoconazole. The later NMR study proved the formation of H-bonding through this carbonyl moiety. The IR spectra of the ketoconazole/HPMC-AS ASD remain unchanged following moisture exposure, presumably due to three reasons: (1) the strong drug–polymer interactions (χ = −1.78, Table 2); (2) the relatively hydrophobic nature of HPMC-AS; (3) the fact that the ketoconazole/HPMC-AS interaction increased the hydrophobicity of the ASD (Figure 3). All above might have facilitated the preservation of the drug–polymer bonding during the moisture exposure and dissolution process, and eventually contributed to the superior dissolution performance of this system, which will be discussed in detail later.

Solution NMR Investigation of the Specific Interaction between Drug and Polymer. To further explore the molecular mechanism of drug–polymer interaction, solution ^{13}C NMR spectra of the pure drug, as well as the drug/polymer combination, were collected and compared.

For the griseofulvin/PVP-VA and griseofulvin/HPMC-AS systems, the chemical shifts of the griseofulvin C atoms remained unchanged compared with those of the pure drug (Table 3), further confirming the absence of drug–polymer interaction in these systems.

For the felodipine/PVP-VA system, addition of PVP-VA apparently influenced the 1,4-dihydropyridine ring on felodipine: the C-3 and C-5 peaks shifted moderately upfield ($\Delta\delta$ = −0.16), and the C-2 and C-6 peaks shifted downfield ($\Delta\delta$ = +0.17) (Table 3). The decrease of electron density in felodipine C-2 and C-6 further confirmed the formation of H-bonding between the −NH group of felodipine with the −C═O (vinyl acetate) of PVP-VA, which was already proved by the FT-IR study (Figure 6).

Similarly in the felodipine/HPMC-AS system, the 1,4-dihydropyridine in felodipine was also affected by the addition of HPMC-AS. Different from the felodipine/PVP-VA system, the C-3 and C-5 peaks shifted slightly downfield ($\Delta\delta$ = +0.13) and the C-2 and C-6 peaks shifted upfield ($\Delta\delta$ = −0.12) (Table 3). The increase of C-2 and C-6 electron density and the decrease of C-3 and C-5 electron density were attributed to the conjugative interaction with the carbonyl group in HPMC-AS, and the possible formation of a dipole–induced dipole complex between the carbonyl groups in HPMC-AS, and the 1,4-dihydropyridine ring in felodipine. A similar complex formation mechanism was reported in the literature.[43]

DOI: 10.1021/mp500660m
Mol. Pharmaceutics 2015, 12, 576–589

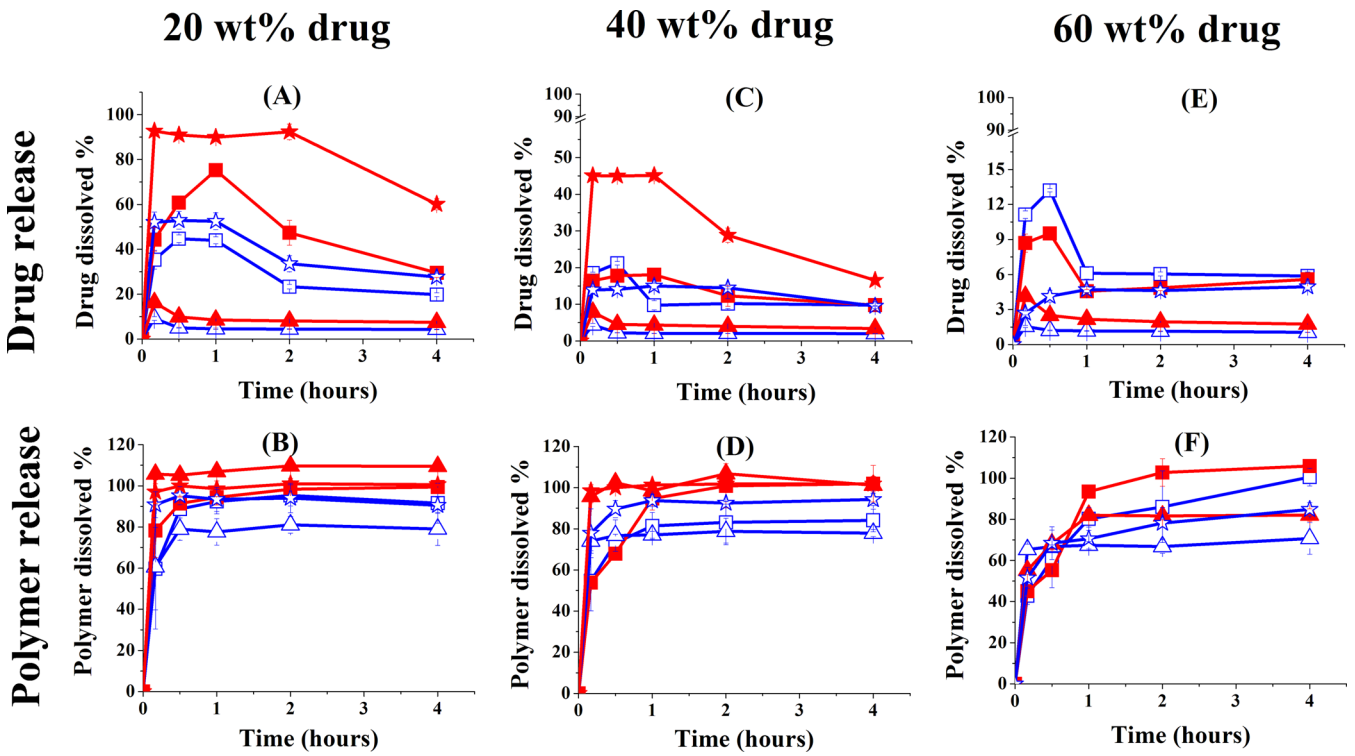

Figure 8. Dissolution of ASDs in FaSSIF solution at the ASD concentration of 5 mg/mL. Both drug and polymer release profiles were measured and are listed on the top (A, C, E) and bottom (B, D, F) panels, respectively. The profiles are arranged according to the drug loading in the ASDs: (A, B) ASD with 20% drug loading; (C, D) ASD with 40% drug loading; (E, F) ASD with 60% drug loading (n = 3 for all experiments) (blue △, G/P ASD; red ▲, G/H ASD; blue □, F/P ASD; red ■, F/H ASD; blue ☆, K/P ASD; red ★, K/H ASD).

In the ketoconazole/PVP-VA system, the ketoconazole C-25 showed a moderate upfield shift ($\Delta\delta$ = −0.17) with the addition of PVP-VA (Table 3), suggesting an elevated electron density on C-25 caused by the approach of positively charged nitrogen atom of the amide group on the PVP-VA pyrrolidone rings. In another words, we conclude that a dipole-induced dipole complex was formed between the amide groups of the PVP-VA pyrrolidone ring and the ketoconazole pyrrole.

In the ketoconazole/HPMC-AS system, the downfield shift of C-2 ($\Delta\delta$ = +0.16) was observed with the addition of HPMC-AS (Table 3), which could be attributed to the H-bonding formation between the ketoconazole carbonyl and HPMC-AS. Besides the shift of the C-2 peak, the peaks assigned to ketoconazole imidazole carbon (C-24, C-25, C26) shifted significantly as HPMC-AS was introduced. Both C-24 and C-25 peaks shifted upfield ($\Delta\delta$ = −0.16 and −0.81, respectively), and the C-26 peak shifted downfield ($\Delta\delta$ = +0.13) (Table 3), which suggest the formation of conjugative interaction and a dipole-induced dipole complex between the ketoconazole imidazole and HPMC-AS carbonyl group.

Drug and Polymer Release Kinetics under Two Different Nonsink Conditions. To have a comprehensive understanding of the dissolution performance of different ASDs, we studied the dissolution kinetics of both the drugs and the polymers from 18 different ASDs, that is, griseofulvin/PVP-VA, griseofulvin/HPMC-AS, felodipine/PVP-VA, felodipine/HPMC-AS, ketoconazole/PVP-VA, and ketoconazole/HPMC-AS, each system including 20%, 40%, and 60% drug loading. We also used different nonsink conditions (i.e., different drug supersaturation) at 0.5 mg/mL and 5 mg/mL ASD concentration to compare the dissolution performance at different dosing strength. Both drug release kinetics and polymer release kinetics were analyzed for each condition. The results are summarized in Figure 7 (0.5 mg/mL ASD concentration) and Figure 8 (5 mg/mL ASD concentration), respectively.

Figure 7A shows the drug dissolution kinetics of the 20% ASDs at a relatively low drug dosing strength at 0.1 mg/mL (0.5 mg/mL ASD concentration, i.e., 25 mg of API dosed in a 250 mL GI volume). Correspondingly, Figure 7B showed the fast and complete polymer dissolution kinetics from the 20% ASDs. Within ∼10 min, polymer concentration reached ∼0.4 mg/mL (i.e., 20:80 drug:polymer ratio, at 0.5 mg/mL ASD concentration) in most ASD systems except for the felodipine/PVP-VA system, wherein polymer released slightly more slowly and the polymer concentration achieved ∼0.3 mg/mL after 10 min. As demonstrated by Figure 7A, drug released from the 20% ketoconazole/PVP-VA and ketoconazole/HPMC-AS ASD similarly and both reached and remained above 85% during the entire 4 h dissolution study; 20% griseofulvin/PVP-VA and griseofulvin/HPMC-AS ASDs also released drug similarly, wherein more than 90% griseofulvin was initially dissolved in the dissolution medium yet the amount of drug gradually decreased to ∼65% after 4 h. Interestingly, drug dissolution from 20% felodipine/PVP-VA and felodipine/HPMC-AS appeared to be very different: 80% felodipine released rapidly from the HPMC-AS ASD after 10 min, and then the amount of dissolved felodipine gradually decreased to ∼55% after 4 h. In contrast, dissolution of felodipine from the PVP-VA ASD was slow and incomplete. Only ∼35% of felodipine dissolved after 4 h.

Figure 7C shows the drug dissolution kinetics of the 40% ASDs at 0.5 mg/mL ASD concentration. Again, fast and complete polymer dissolution from most ASDs was observed,

DOI: 10.1021/mp500660m
Mol. Pharmaceutics 2015, 12, 576−589

and the felodipine/PVP-VA system showed a slight yet noticeable, slower initial polymer dissolution rate (Figure 7D). Nevertheless, polymer concentration in all systems approached ~0.3 mg/mL (i.e., 40:60 drug:polymer ratio, at 0.5 mg/mL ASD concentration) after 1 h. In terms of drug release kinetics, the 40% ketoconazole/HPMC-AS system was the one ASD that released ~100% of the drug and maintained the drug concentration over 4 h, significantly outperforming the ketoconazole/PVP-VA ASD that gradually released ~35% drug over 4 h. In the first 1 h, drug dissolution from the griseofulvin/HPMC-AS and felodipine/HPMC-AS ASDs was faster than that from their PVP-VA counterparts; while between 1 and 4 h, polymer type did not affect the dissolved drug concentration in either griseofulvin or felodipine ASD systems, which was between 20 and 40%. With further increase of the ASD drug loading to 60% and decrease of the polymer to 40%, the drug and polymer dissolution kinetics from the ASDs are summarized in Figure 7E and 7F. The only ASD that still showed significant drug dissolution was the ketoconazole/HPMC-AS system. Overall, the HPMC-AS ASDs again outperformed the PVP-VA systems in the first 1 h, while the drug dissolution of all but ketoconazole/HPMC-AS ASDs decreased to ~20% and was maintained within 1−4 h, regardless of the polymer type.

Figure 8 is essentially a replica of the study in Figure 7, except that the ASD dosing strength was increased 10 times, from 0.5 mg/mL to 5 mg/mL. The 20%, 40%, and 60% ASD correspond to 250, 500, or 750 mg doses, respectively, assuming 250 mL GI volume. With this study, we hope to understand the impact of the API dose and level of supersaturation on the dissolution performance of ASDs.

In comparison of Figures 7 and 8, we determined and summarized the *dissolution performance parameters* of all the solid dispersions under different dissolution conditions, and listed them together with others major findings, including drug crystallization tendency, drug−polymer interaction, *supersaturation parameter*, etc., in Table 4. In summary, we have the following observations:

1. For all systems, HPMC-AS ASDs showed drug dissolution performance that was superior, or at least similar, to that of the corresponding PVP-VA ASDs, regardless of the dosing strength, or drug loading in the ASD (Table 4, "dissolution performance parameter").
2. PVP-VA or HPMC-AS completely dissolved when the dose and the ASD drug loading were low (Figure 7B,D). Incomplete polymer release was observed when the drug loading was high (Figure 7F), or dose was high (Figure 8B,D), or both (Figure 8F). Regardless of dose or drug loading, HPMC-AS usually dissolves faster and more completely than PVP-VA, or at least similarly (compare the red, HPMC-AS dissolution profiles, with the blue, PVP-VA profiles, in Figures 7B,D,F and 8B,D,F). This could due to the intrinsic dissolution rates of these two polymers, as well as the crystallization of the drugs within the polymers. Water penetrates the PVP-VA ASD more readily compared with the HPMC-AS ASD, which could induce more drug crystallization within the PVP-VA system. The crystallized drugs could serves as insoluble "bricks" to prevent the release of polymer. This could have occurred in the relatively hydrophilic felodipine/PVP-VA system.

Table 4. A Summarization of Key Physiochemical Characters, Different Interactions in ASDs, and the Corresponding ASD Dissolution Performance[a]

	drug−polymer interaction in solid state					supersaturation parameter of polymers				dissolution performance parameter							
						0.2 mg/mL drug		1 mg/mL drug		0.5 mg/mL ASD				5 mg/mL ASD			
ASD	crystn tendency in soln/solid[b]	FH interaction, χ	H-bonding formation by FT-IR (Y/N)	drug−polymer interaction by NMR	disruption of drug−polymer interaction by water?	0.3 mg/mL[c]	3 mg/mL[c]	0.3 mg/mL[c]	3 mg/mL[c]	20[d]	40[d]	60[d]	20[d]	40[d]	60[d]
G/P	H/(class I)	W	N	no interaction	N/A	0.27	0.22	0.03	0.10	0.75	0.23	0.14	0.05	0.02	0.01
G/H	H/(class I)	W	N	no interaction	N/A	0.17	0.41	0.05	0.10	0.73	0.29	0.21	0.09	0.04	0.02
F/P	M/(class III)	S	Y	H-bonding	N	0.51	0.73	0.04	0.35	0.33	0.31	0.20	0.29	0.11	0.07
F/H	M/(class III)	M	Y	dipole complex (W)	Y	0.40	0.73	0.07	0.41	0.62	0.37	0.18	0.48	0.13	0.06
K/P	L/(class III)	M	N	dipole complex (M)	Y	0.36	0.30	0.27	0.17	0.85	0.28	0.15	0.38	0.13	0.04
K/H	L/(class III)	S	Y	H-bonding and dipole complex (S)	N	0.57	0.65	0.23	0.49	0.95	0.97	0.80	0.82	0.31	0.15

[a]Abbreviations: G (griseofulvin), F (felodipine), K (ketoconazole), P (PVP-VA), H (HPMC-AS), W (weak), M (medium), S (strong), N (no), Y (yes), N/A (not applicable), L (low), H (high). [b]Classification of crystallization tendency of amorphous drug in FaSSIF: high if drug crystallized within 30 min, low if drug did not crystallize within 4 h, and medium if drug crystallized between 30 min and 4 h. Crystallization tendency in the solid state is classified according to Baird et al.[37] [c]Polymer concentration. [d]Drug loading (%).

DOI: 10.1021/mp500660m
Mol. Pharmaceutics 2015, 12, 576−589

3. Ketoconazole/HPMC-AS ASD performed strikingly better than any other ASDs, including the ketoconazole/PVP-VA system (Table 4). The fact that ketoconazole/HPMC-AS performed so much better than ketoconazole/PVP-VA in various dissolution conditions might have suggested that, besides the low intrinsic crystallization tendency of ketoconazole (Figure 4), other factors, including (a) the strong drug−polymer interaction (Table 2), (b) the physical nature of the ketoconazole/HPMC-AS interaction that increased the hydrophobicity of this ASD (Figure 3), (c) the robustness of the ketoconazole/HPMC-AS interaction that was able to survive the moisture exposure (Figure 6), (d) the fast dissolution kinetics of HPMC-AS (Figures 7, 8), and (e) the ability of HPMC-AS to maintain a higher supersaturation of ketoconazole (Table 4, "supersaturation parameter"), might have collectively and interdependently contributed to this performance.
4. At high dose or high drug loading, griseofulvin ASDs were unable to provide sufficient griseofulvin dissolution, regardless of the polymer type (Table 4). Apparently, for a fast crystallizer like griseofulvin that has no strong interaction with polymer carriers (Table 2), decreasing the ASD drug loading could be the only option to improve the drug dissolution, and only at low drug dose. It would be interesting to identify other fast crystallizers that interact strongly with polymers, and to carry on similar investigations.
5. The dissolution performance of different ASDs remains individualized. It is very difficult to predict the dissolution performance of ASDs by any single commonly used assay, such as drug−polymer interaction assessment in the solid state, or drug supersaturation in the presence of different polymers, etc. For instance, HPMC-AS and PVP-VA were able to maintain the supersaturation of felodipine similarly (Figures 5C and 5D and Table 4, "supersaturation parameter"), and felodipine interacts more strongly with PVP-VA than HPMC-AS (Table 2). However, felodipine/HPMC-AS outperformed or at least tied with felodipine/PVP-VA ASDs in all dissolution conditions (Figures 7 and 8 and Table 4, "dissolution performance parameter").

Key physiochemical properties related to the performance of an ASD system are listed in Table 4. These key properties include the crystallization tendency of the drug in aqueous medium, drug−polymer interaction in dry state and in aqueous medium, the drug dose, the drug loading in the ASD, and the amount of polymer that is available to maintain drug supersaturation in solution (i.e., the polymer dissolution rate). We conclude that the dissolution performance of ASDs was jointly influenced by all these factors and, fundamentally, the interaction between drug, polymer, and water. Obviously, one could conclude that further mechanistic and comprehensive investigation into these systems is required to decode the dissolution mechanism of the ASD systems and to predict the *in vitro* and, eventually, *in vivo* performance. The definition of two quantitative parameters, the *supersaturation parameter* and the *dissolution performance parameter*, was found to be highly valuable to compare different drug−polymer systems. As pointed out earlier, these parameters are functions of multiple complicated and potentially interrelated physical processes. The exact correlations between them are still under continued investigation in our lab and will be discussed in the future.

AUTHOR INFORMATION

Corresponding Author

*E-mail:qianfeng@biomed.tsinghua.edu.cn.

Notes

The authors declare no competing financial interest.

ACKNOWLEDGMENTS

F.Q. acknowledges the start-up funds provided by the *Center for Life Sciences at Tsinghua and Peking Universities* (Beijing, China), and by the *China Recruitment Program of Global Experts* to establish the research laboratory. Y.C. thanks Bristol-Myers Squibb Company (Lawrenceville, NJ, USA) for providing a Ph.D. fellowship to support her Ph.D. research. The authors thank Prof. Lian Yu (School of Pharmacy, University of Wisconsin, Madison) for helpful discussion regarding the determination of Flory−Huggins parameters.

REFERENCES

(1) Hancock, B. C. Disordered drug delivery: Destiny, dynamics and the Deborah number. *J. Pharm. Pharmacol.* **2002**, *54*, 737−46.

(2) Ediger, M. D.; Angell, C. A.; Nagel, S. R. Supercooled liquids and glasses. *J. Phys. Chem.* **1996**, *100* (31), 13200−13212.

(3) Hancock, B. C.; Zografi, G. Characteristics and significance of the amorphous state in pharmaceutical systems. *J. Pharm. Sci.* **1997**, *86* (1), 1−12.

(4) Yu, L. Amorphous pharmaceutical solids: preparation, characterization and stabilization. *Adv. Drug Delivery Rev.* **2001**, *48* (1), 27−42.

(5) Zhou, D.; Zhang, G. G. Z.; Law, D.; Grant, D. J. W.; Schmitt, E. A. Physical stability of amorphous pharmaceuticals: Importance of configurational thermodynamic quantities and molecular mobility. *J. Pharm. Sci.* **2002**, *91* (8), 1863−1872.

(6) Graeser, K. A.; Patterson, J. E.; Zeitler, J. A.; Gordon, K. C.; Rades, T. Correlating thermodynamic and kinetic parameters with amorphous stability. *Eur. J. Pharm. Sci.* **2009**, *37* (3−4), 492−8.

(7) Aso, Y.; Yoshioka, S.; Kojima, S. Explanation of the crystallization rate of amorphous nifedipine and phenobarbital from their molecular mobility as measured by ^{13}C nuclear magnetic resonance relaxation time and the relaxation time obtained from the heating rate dependence of the glass transition temperature. *J. Pharm. Sci.* **2001**, *90* (6), 798−806.

(8) Murdande, S. B.; Pikal, M. J.; Shanker, R. M.; Bogner, R. H. Solubility advantage of amorphous pharmaceuticals: I. A thermodynamic analysis. *J. Pharm. Sci.* **2010**, *99* (3), 1254−1264.

(9) Murdande, S. B.; Pikal, M. J.; Shanker, R. M.; Bogner, R. H. Solubility advantage of amorphous pharmaceuticals: II. Application of quantitative thermodynamic relationships for prediction of solubility enhancement in structurally diverse insoluble pharmaceuticals. *Pharm. Res.* **2010**, *27* (12), 2704−14.

(10) Murdande, S. B.; Pikal, M. J.; Shanker, R. M.; Bogner, R. H. Solubility advantage of amorphous pharmaceuticals, part 3: Is maximum solubility advantage experimentally attainable and sustainable? *J. Pharm. Sci.* **2011**, *100* (10), 4349−4356.

(11) Qian, F.; Huang, J.; Hussain, M. A. Drug-polymer solubility and miscibility: Stability consideration and practical challenges in amorphous solid dispersion development. *J. Pharm. Sci.* **2010**, *99* (7), 2941−2947.

(12) Taylor, L. S.; Zografi, G. Sugar−polymer hydrogen bond interactions in lyophilized amorphous mixtures. *J. Pharm. Sci.* **1998**, *87* (12), 1615−1621.

(13) Marsac, P. J.; Konno, H.; Taylor, L. S. A comparison of the physical stability of amorphous felodipine and nifedipine systems. *Pharm. Res.* **2006**, *23* (10), 2306−16.

DOI: 10.1021/mp500660m
Mol. Pharmaceutics 2015, 12, 576−589

(14) Taylor, L. S.; Zografi, G. Spectroscopic characterization of interactions between PVP and indomethacin in amorphous molecular dispersions. *Pharm. Res.* **1997**, *14* (12), 1691−98.
(15) Konno, H.; Taylor, L. S. Influence of different polymers on the crystallization tendency of molecularly dispersed amorphous felodipine. *J. Pharm. Sci.* **2006**, *95* (12), 2692−705.
(16) Konno, H.; Taylor, L. S. Ability of different polymers to inhibit the crystallization of amorphous felodipine in the presence of moisture. *Pharm. Res.* **2008**, *25* (4), 969−78.
(17) Khougaz, K.; Clas, S.-D. Crystallization inhibition in solid dispersions of MK-0591 and poly(vinylpyrrolidone) polymers. *J. Pharm. Sci.* **2000**, *89* (10), 1325−1334.
(18) Rumondor, A. C. F.; Taylor, L. S. Effect of polymer hygroscopicity on the phase behavior of amorphous solid dispersions in the presence of moisture. *Mol. Pharmaceutics* **2010**, *7* (2), 477−90.
(19) Jackson, M. J.; Toth, S. J.; Kestur, U. S.; Huang, J.; Qian, F.; Hussain, M. A.; Simpson, G. J.; Taylor, L. S. Impact of polymers on the precipitation behavior of highly supersaturated aqueous danazol solutions. *Mol. Pharmaceutics* **2014**, *11* (9), 3027−38.
(20) Rumondor, A. C. F.; Marsac, P. J.; Stanford, L. A.; Taylor, L. S. Phase behavior of poly(vinylpyrrolidone) containing amorphous solid dispersions in the presence of moisture. *Mol. Pharmaceutics* **2009**, *6* (5), 1492−1505.
(21) Marsac, P. J.; Rumondor, A. C.; Nivens, D. E.; Kestur, U. S.; Stanciu, L.; Taylor, L. S. Effect of temperature and moisture on the miscibility of amorphous dispersions of felodipine and poly(vinyl pyrrolidone). *J. Pharm. Sci.* **2010**, *99* (1), 169−85.
(22) Vasanthavada, M.; Tong, W.-Q.; Joshi, Y.; Kislalioglu, M. S. Phase behavior of amorphous molecular dispersions II: Role of hydrogen bonding in solid solubility and phase separation kinetics. *Pharm. Res.* **2005**, *22* (3), 440−448.
(23) Qian, F.; Wang, J.; Hartley, R.; Tao, J.; Haddadin, R.; Mathias, N.; Hussain, M. Solution behavior of PVP-VA and HPMC-AS-Based amorphous solid dispersions and their bioavailability implications. *Pharm. Res.* **2012**, *29* (10), 2765−76.
(24) Newman, A.; Knipp, G.; Zografi, G. Assessing the performance of amorphous solid dispersions. *J. Pharm. Sci.* **2012**, *101* (4), 1355−77.
(25) Friesen, D. T.; Shanker, R.; Crew, M.; Smithey, D. T.; Curatolo, W. J.; Nightingale, J. A. S. Hydroxypropyl methylcellulose acetate succinate-based spray-dried dispersions: An overview. *Mol. Pharmaceutics* **2008**, *5* (6), 1003−1019.
(26) Ilevbare, G. A.; Taylor, L. S. Liquid−liquid phase separation in highly supersaturated aqueous solutions of poorly water-soluble drugs: Implications for solubility enhancing formulations. *Cryst. Growth Des.* **2013**, *13* (4), 1497−1509.
(27) Alonzo, D. E.; Zhang, G. G.; Zhou, D.; Gao, Y.; Taylor, L. S. Understanding the behavior of amorphous pharmaceutical systems during dissolution. *Pharm. Res.* **2010**, *27* (4), 608−18.
(28) Alonzo, D. E.; Gao, Y.; Zhou, D.; Mo, H.; Zhang, G. G.; Taylor, L. S. Dissolution and precipitation behavior of amorphous solid dispersions. *J. Pharm. Sci.* **2011**, *100* (8), 3316−31.
(29) Ilevbare, G. A.; Liu, H.; Edgar, K. J.; Taylor, L. S. Maintaining supersaturation in aqueous drug solutions: Impact of different polymers on induction times. *Cryst. Growth Des.* **2013**, *13* (2), 740−751.
(30) Alonzo, D. E.; Raina, S.; Zhou, D.; Gao, Y.; Zhang, G. G. Z.; Taylor, L. S. Characterizing the impact of hydroxypropylmethyl cellulose on the growth and nucleation kinetics of felodipine from supersaturated solutions. *Cryst. Growth Des.* **2012**, *12* (3), 1538−1547.
(31) Simonelli, A. P.; Mehta, S. C.; Higuchi, W. I. Dissolution rates of high energy polyvinylpyrrolidone(PVP) sulfathiazole coprecipitates. *J. Pharm. Sci.* **1969**, *58*, 538−549.
(32) Sun, Y.; Tao, J.; Zhang, G. G.; Yu, L. Solubilities of crystalline drugs in polymers: An improved analytical method and comparison of solubilities of indomethacin and nifedipine in PVP, PVP/VA, and PVAc. *J. Pharm. Sci.* **2010**, *99* (9), 4023−31.
(33) Zhang, J.; Zografi, G. The relationship between "BET"- and "Free volume"-Derived parameters for water vapor absorption into amorphous solids. *J. Pharm. Sci.* **2000**, *89* (8), 1063−1072.
(34) Hancock, B. C.; Zografi, G. The use of solution theories for predicting water vapor absorption by amorphous pharmaceutical solids: A test of the Flory-Huggins and Vrentas Models. *Pharm. Res.* **1993**, *10* (9), 1262−1267.
(35) Van den Mooter, G.; Wuyts, M.; Blaton, N.; Busson, R.; Grobet, P.; Augustijns, P.; Kinget, R. Physical stabilisation of amorphous ketoconazole in solid dispersions with polyvinylpyrrolidone K25. *Eur. J. Pharm. Sci.* **2001**, *12* (3), 261−269.
(36) Jung, J.; Kim, L.; Lee, C. S.; Cho, Y. H.; Ahn, S.-H.; Lim, Y. Total assignment of the ^{1}H and ^{13}C NMR data for felodipine and its derivatives. *Magn. Reson. Chem.* **2001**, *39* (7), 406−410.
(37) Baird, J. A.; Van Eerdenbrugh, B.; Taylor, L. S. A classification system to assess the crystallization tendency of organic molecules from undercooled melts. *J. Pharm. Sci.* **2010**, *99* (9), 3787−806.
(38) Zhou, D.; Zhang, G. G. Z.; Law, D.; Grant, D. J. W.; Schmitt, E. A. Thermodynamics, molecular mobility and crystallization kinetics of amorphous griseofulvin. *Mol. Pharmaceutics* **2008**, *5* (6), 927−936.
(39) Klug, D. D. Thermodynamics. Glassy water. *Science* **2001**, *294* (5550), 2305−6.
(40) Bevernage, J.; Forier, T.; Brouwers, J.; Tack, J.; Annaert, P.; Augustijns, P. Excipient-mediated supersaturation stabilization in human intestinal fluids. *Mol. Pharmaceutics* **2011**, *8* (2), 564−70.
(41) Huggins, M. L. Thermodynamic properties of solutions of long-chain compounds. *Ann. N.Y. Acad. Sci.* **1942**, *43* (1), 1−32.
(42) Flory, P. J. Thermodynamics of high polymer solutions. *J. Chem. Phys.* **1942**, *10* (1), 51−61.
(43) Hosono, T.; Tsuchiya, S.; Matsumaru, H. Model of interaction of ajmaline with polyvinylpyrrolidone. *J. Pharm. Sci.* **1980**, *69* (7), 824−826.

DOI: 10.1021/mp500660m
Mol. Pharmaceutics 2015, 12, 576−589